J Nanopart Res (2024) 26:280
https://doi.org/10.1007/s11051-024-06187-w

RESEARCH

A plug-and-play strategy for agrochemical delivery using a plant virus nanotechnology

Adam A. Caparco · Ivonne González-Gamboa · Sabrina Chang-Liao · Nicole F. Steinmetz

Received: 25 August 2024 / Accepted: 18 November 2024 / Published online: 14 December 2024

Abstract Delivery of agrochemicals into soil presents a challenge, as the active ingredients are often hydrophobic and do not possess adequate soil mobility to reach their target pest. Previously, plant virus nanoparticles have been shown to penetrate soil and deliver agrochemicals for the treatment of plant parasitic nematodes. For example, tobacco mild green mosaic virus (TMGMV) can be functionalized with agrochemicals through bioconjugation, infusion at the coat protein interface, or encapsulation through thermal shapeshifting (rod-to-sphere). There continues to be a need to expand approaches for agrochemical display and delivery with a need for plug-and-play technology to be applicable for multiple nanoparticle platforms and agrochemicals. Toward this goal, we turned toward a bio-specific coupling strategy making use of the biotin-(strept)avidin system. Herein, we conjugated TMGMV with either avidin or biotin using azide-alkyne cycloaddition. The avidin/biotin-functionalized TMGMV nanoparticles were then characterized by gel electrophoresis and

Supplementary Information The online version contains supplementary material available at https://doi.org/10.1007/s11051-024-06187-w.

A. A. Caparco · I. González-Gamboa · S. Chang-Liao · N. F. Steinmetz (✉)
Aiiso Yufeng Li Family Department of Chemical and Nano Engineering, University of California San Diego, 9500 Gilman Dr, La Jolla, CA 92093, USA
e-mail: nsteinmetz@ucsd.edu

A. A. Caparco · I. González-Gamboa · S. Chang-Liao · N. F. Steinmetz
Center for Nano-ImmunoEngineering, University of California San Diego, 9500 Gilman Dr, La Jolla, CA 92093, USA

A. A. Caparco · I. González-Gamboa · S. Chang-Liao · N. F. Steinmetz
Shu and K.C. Chien and Peter Farrell Collaboratory, University of California San Diego, 9500 Gilman Dr, La Jolla, CA 92093, USA

I. González-Gamboa
Department of Molecular Biology, University of California San Diego, 9500 Gilman Dr, La Jolla, CA 92093, USA

N. F. Steinmetz
Department of Bioengineering, University of California San Diego, 9500 Gilman Dr, La Jolla, CA 92093, USA

N. F. Steinmetz
Department of Radiology, University of California San Diego, 9500 Gilman Dr, La Jolla, CA 92093, USA

N. F. Steinmetz
Center for Engineering in Cancer, Institute of Engineering in Medicine, University of California San Diego, 9500 Gilman Dr, La Jolla, CA 92093, USA

N. F. Steinmetz
Moores Cancer Center, University of California, University of California San Diego, 9500 Gilman Dr, La Jolla, CA 92093, USA

N. F. Steinmetz
Institute for Materials Discovery and Design, University of California San Diego, 9500 Gilman Dr, La Jolla, CA 92093, USA

electron microscopy to confirm cargo loading and the nanoparticle's structural integrity. Soil column assays confirmed that soil mobility was maintained upon chemical modification. Ivermectin modified with biotin or streptavidin linkers was then introduced to the TMGMV-avidin/biotin nanoparticles and binding propensity and loading were validated by QCM-D and a competitive ELISA. Finally, the ivermectin-loaded TMGMV nanoparticles were used to treat *C. elegans* in a gel burrowing assay, demonstrating that either pesticide loading strategy resulted in active TMGMV nanoparticle formulation that significantly reduced the mobility of nematodes, even after passing through soil. In stark contrast, free ivermectin only exhibited efficacy when applied directly to nematodes; the free pesticide was lost in the soil column—highlighting the need for a delivery system. The presented approach provides a facile plug-and-play approach for pesticide loading onto TMGMV nanoparticles. In particular, biotinylated TMGMV with streptavidin-conjugated ivermectin served as the most effective formulation. Importantly this method does not require heat, which contrasts our previous method of thermal reshaping that requires sample and pesticide exposure to temperatures > 96 °C. We envision the bio-specific loading strategy could be extended to other protein or inorganic nanoparticles to advance soil treatment strategies.

Keywords Nanopesticides · Agrochemicals · Ivermectin · Tobacco mild green mosaic virus · Nematodes

Introduction

Delivery of agrochemicals through the soil presents unique challenges. Many agrochemicals are hydrophobic, with low aqueous solubilities and poor mobility in the soil [1, 2]. This bears a hurdle to effective treatment of pests residing at the roots of plants, such as plant parasitic nematodes which are detrimental to food security and the economics of growing crops [1, 3, 4]. To circumvent this delivery challenge, agrochemicals (nematicides) are often applied at high doses with large doses being lost in the environment, leaching into the groundwater and causing health risks to humans and livestock [1, 4–6]. Using the principles of nanomedicine to target the delivery of these compounds presents an opportunity to improve the sustainability of agricultural practices and the efficacy of these agrochemicals where they are needed [7].

Nanoparticles have the potential to address the delivery challenge in agriculture. Polymeric nanocarriers and metallic nanoparticles have been used to promote nutrient uptake and pest management [2, 8, 9]. Our approach centers on plant viruses—proteinaceous nanoparticles which share the soil environment with nematodes. There are many classes of plant viruses, some of which are known to be carried by nematodes as vectors, such as nepoviruses and those transmitted by Longidoridae and Trichodoridae nematodes [9–15]. By selecting a plant virus with demonstrated soil mobility yet a limited host range of plants, we can repurpose the biology to turn the virus into a nanocarrier for targeted treatment of nematodes at minimal risk to the environment and agriculturally relevant plants [7, 16]. To date, red clover necrotic mosaic virus (RCNMV) and tobacco mild green mosaic virus (TMGMV) have been developed for agrochemical delivery, i.e., delivery of ivermectin for treatment of plant parasitic nematodes [11, 17–19]. Using RCNMV, nematicide loading was achieved through ion-dependent gating mechanisms [12], and in the case of TMGMV, covalent loading strategies [20] as well as non-covalent strategies (infusion at the coat protein interface and thermal reshaping of TMGMV rods-to-spheres) were pursued to load ivermectin as well as other pesticides [17, 21].

There continues to be a need to expand approaches for agrochemical display and delivery with a need for plug-and-play technology to be applicable for multiple nanoparticle platforms and agrochemicals. In particular, for adoption in an agricultural setting, fewer processing steps, ease of use, and low cost of preparation are essential for a technology to take root. However, some facile techniques do not achieve the desired efficacy to overcome delivery challenges in agriculture. For example, the infusion technique—where pesticides are loaded at the coat protein (CP) interface—is limited to what type of compounds could be loaded, and while the design rules are yet to be elucidated, size, geometry, charge, and polarity play a role [10, 21]. While the thermal shape-shifting method yielded spherical TMGMV nanoparticles with high pesticide encapsulation efficiency [14], this method is limited to heat-stable compounds. Therefore, we explored a bio-specific coupling strategy

making use of the well-established biotin-(strept)avidin system. Herein, ivermectin was used as a model pesticide and modified either with biotin or streptavidin for coupling to TMGMV modified with the corresponding avidin or biotin linker. The degree of pesticide loading was quantified using quartz crystal microbalance with dissipation monitoring (QCMD) and competitive ELISA. Pesticide-loaded TMGMV particles were passed through soil to confirm their mobility and retention of the agrochemicals, and then the samples were used to treat *C. elegans* (as a model system). In aggregate, this system serves as a method to associate hydrophobic cargo that is not amenable to thermal transformation or conjugation to plant virus nanoparticles.

Experimental methods

Preparation of TMGMV

TMGMV (BioProdex; FL, USA) was purified using established protocols [22]. Briefly, TMGMV was dialyzed against 10 mM potassium phosphate buffer (pH 7.4) (KP) for 24 h under constant stirring using a 10-kDa MWCO Slide-A-Lyzer dialysis membrane (Thermo Scientific; MA, USA). The solution was exchanged for fresh buffer and dialyzed for another 48 h. The retentate was transferred to centrifuge tubes and centrifuged at 10,000 × g for 20 min at 4 °C (Beckman Coulter Allegra; CA, USA). The supernatant was transferred to a new tube and the centrifugation was repeated. The supernatant was transferred to an ultracentrifugation tube and spun down for 3 h at 253,000 × g at 4 °C with a sucrose cushion (30% w/v) (Beckman Coulter Optima L-90 k Ultracentrifuge with 50.2 Ti rotor; CA, USA). The pellet was isolated and resuspended overnight in KP via rocking at 4 °C before quantification of concentration by UV–Vis using a Nanodrop 2000 (Thermo Scientific; MA, USA).

Preparation of avidin-azide

Avidin (Lee Biosolution; MO, USA) was dissolved into 0.1 M sodium carbonate (pH 9) at 20 mg mL^{-1}. *N*-Hydroxysuccinimide-azide (NHS-N_3; Thermo Scientific; MA, USA) dissolved in DMSO was added to the avidin solutions at 2:1, 1:1, 1:2, and 1:4 ratio of reactive NHS groups per lysine on avidin (containing 9 lysine per monomer) and reacted at room temperature for 30 min, 1 h, 2 h, and 24 h. The products were purified using a dialysis membrane (Thermo Scientific; MA, USA) with a molecular weight cutoff value of 3000 Daltons for 48 h against 25 mM HEPES buffer (pH 7.5) and stored at 4 °C.

Preparation of TMGMV-alkyne

Diazonium salts were prepared as described previously using 4-ethynylaniline and *p*-toluenesulfonic acid with sodium nitrite (Sigma-Aldrich; MO, USA) [22]. TMGMV was diluted to 2 mg mL^{-1} in 100 mM borate buffer (pH 8.5). The diazonium salt solution was added to the TMGMV solution at 8% final volume (with about twofold molar excess diazonium to TMGMV coat protein) and mixed by inversion before reacting on ice for 30 min. TMGMV samples were isolated by centrifugation at 169,000 × g using a tabletop ultracentrifuge (Beckman Optima MAX-XP with TLA-55 rotor) for 1 h over a sucrose cushion (30% w/v). The TMGMV pellet was resuspended in KP overnight at 4 °C on a rotary shaker.

Preparation of ivermectin-biotin and ivermectin-streptavidin conjugates

Ivermectin conjugates were custom synthesized by KareBay Biochem (NJ, USA). Briefly, the conjugates were prepared with a 4-kDa polyethylene glycol linker such that the conjugation would be less likely to affect biological activity. Biotin was linked to ivermectin via the valeric acid moiety, and streptavidin was linked to ivermectin via a surface-accessible lysine residue.

Preparation of TMGMV-biotin and TMGMV-avidin

The reaction conditions were modeled after our previous work [22]. In an ultracentrifugation tube (Beckman Coulter 357,448; IN, USA), 1 mg of TMGMV-alkyne was added to 2 mM aminoguanidine, 1 mM copper sulfate pre-mixed with 3.7 mM tris(benzyltriazolylmethyl) amine (Sigma-Aldrich; MO, USA), and 2 mM L-ascorbic acid (the addition of compounds was in that order) [22]. The molar ratio of reactive azides (biotin-N_3 or avidin-N_3) per TMGMV coat protein was varied (2:1, 1:1, and 1:2

ratio of avidin per CP), and the final volume was 500 µL. The click reaction occurred on ice for 1 h. A 200-µL sucrose cushion (30% w/v) was added and the samples were purified by ultracentrifugation as described above. The supernatant was removed, and the pellet was resuspended in 20 mM HEPES in the ultracentrifugation tube under rotational mixing at 4 °C overnight before being stored at 4 °C. The products were denoted as follows: TMGMV labeled with biotin is TMGMV-B and TMGMV labeled with avidin is TMGMV-A.

Transmission electron microscopy

Samples were diluted to the concentration of 0.05 mg mL^{-1} in deionized water and absorbed onto carbon-coated TEM grids (Electron Microscopy Sciences). The grids were washed three times with DI H_2O and stained by 2% (w/v) uranyl acetate for 2 min. A FEI Tecnai F30 transmission electron microscope operated at 300 kV was used for imaging.

SDS-PAGE

Protein samples were diluted to 10 µg and in 20 µL of buffer or DI H_2O. An aliquot of 4 µL of reducing Laemmli SDS sample buffer, 6X (Thermo Scientific; MA, USA) was added to the solution and mixed. The samples were loaded on a 10-well NuPAGE 12% Bis–Tris SDS-PAGE gel (Thermo Scientific; MA, USA), and electrophoresis was performed in NuPAGE MOPS (1X) buffer for 60 min at 100 V. The gels were either stained in GelCode Blue Stain Reagent (Thermo Scientific; MA, USA) or used for Western blots. For imaging, a gel imager (ProteinSimple; CA, USA) was used. Band intensity analysis in ImageJ was used to determine the relative proportion of native versus modified coat protein, to determine the labeling density of avidin and biotin per TMGMV particle.

Western blots detection of avidin and biotin bound to TMGMV

TMGMV, TMGMV-B, TMGMV-A, avidin, and avidin-N_3 were separated on NuPAGE 12% Bis–Tris SDS-PAGE gels and then transferred onto a nitrocellulose membrane (Thermo Scientific; MA, USA) using NuPAGE Transfer Buffer (Life Technologies; CA, USA). The membrane was then blocked overnight at 4 °C using 0.1 M tris-buffered saline (TBS, pH 7.6) containing 5% (w/v) skim milk powder. For detection of biotin, an anti-biotin horseradish peroxidase (anti-biotin HRP) antibody (Sigma-Aldrich, dilution 1:10,000) was added in TBS for 30 min, followed by washing for 30 min in TBS. The membrane was transferred to a solution of 1-Step TMB ELISA substrate solution (Thermo Scientific; MA, USA) and reacted for 15 min before detecting signals using a gel imager (ProteinSimple; CA, USA). For detection of avidin, the blocked membranes were incubated in sulfo-cyanine 5-biotin (biotin-Cy5) (0.05 mg mL^{-1}; LumiProbe; MD, USA) in TBS for 30 min and then washed for 30 min in TBS, followed by imaging.

Electrophoretic mobility shift assay

All samples were mixed for 30 min prior to electrophoresis and contained 0.5 mg TMGMV in 10 mM KP. TMGMV-B was mixed with equimolar amounts of avidin, and TMGMV-A was mixed with equimolar amounts of 4-arm PEG-Biotin (MW PEG 2 k; Creative PEGWorks; NC, USA). Samples were prepared in KP. All samples were loaded onto a 0.8% (wt/v) agarose gel with GelRed nucleic acid stain diluted 1:10,000 (Biotium; CA, USA) at 25 µg protein per well. The gel was run at 120 V for 40 min before detection of nucleic acid stain by the fluorescent imager (Protein Simple; CA, USA).

Binding of biotin or streptavidin-functionalized ivermectin to TMGMV-A and TMGMV-B

Ivermectin (BioVision; CA, USA) and ivermectin-biotin/streptavidin conjugates (KareBay Biochem; NJ, USA) were mixed using 0.5 mg of TMGMV or TMGMV-B or TMGMV-A in KP at concentrations of 0–10 µM for 30 min at room temperature. The ivermectin-biotin/streptavidin were mixed at an equimolar ratio of binding groups per TMVGMV-A/B and ivermectin. Non-modified TMGMV (0.5 mg) was mixed at an equimolar ratio of ivermectin as a control. Due to the exceptional affinity of avidin and streptavidin for biotin, 1:1 loading of target ivermectin per (strept)avidin/biotin pair was assumed to be an upper limit of binding efficiency.

Competitive ELISA for ivermectin quantification

ELISA for ivermectin quantification was completed as previously described [17] and according to the manufacturer's protocols using a High-Sensitivity Ivermectin ELISA kit (Creative Diagnostics DEIASL215; NY, USA). Absorbance was measured on a plate reader (Tecan Infinite M Plex; CA, USA) at 450 nm, and concentrations were fitted to a standard curve of ivermectin. For ivermectin on TMGMV, TMGMV-A, and TMGMV-B, these results were then compared to the theoretical upper limit determined by band intensity analysis.

Soil mobility of TMGMV and its bioconjugates

Soil mobility of TMGMV, TMGMV-A, and TMGMV-B were quantified using the protein concentration in the elution fractions of a 10-mL Magic Topsoil column as previously described (a more detailed analysis of Magic Topsoil is shown in Table S1). [13, 17]. Briefly, the column was packed vertically, and soil was retained using a water-permeable mesh at the bottom of the column. The column was prewetted with deionized water and excess water was collected in a waste beaker. A constant flowrate of 5 mL min^{-1} of DI H_2O was used to irrigate the samples after 1 mg of TMGMV formulations were loaded from the top and allowed to permeate by gravity into the vertical column. 1.5-mL fractions were collected in microcentrifuge tubes, residual soil sediments were removed by centrifugation, and the supernatant was diluted by eightfold for subsequent spectroscopic analysis. Relative protein concentrations of each fraction were measured by bicinchoninic acid (BCA) Protein Assay (Thermo Scientific; MA, USA) using a Tecan Infinite 200Pro plate reader at 562 nm, and the relative protein concentrations were fitted according to a bovine serum albumin standard curve. Studies were repeated with ivermectin-coated TMGMV particles for further assays.

Quartz crystal microbalance with dissipation (QCM-D) binding assays

Quartz crystal microbalance with dissipation analysis was conducted using a QSense Explore (Biolin Scientific; Stockholm, Sweden). Detection was conducted using a cleaned gold sensor, treated with UV and 3.6% ammonia (v/v)/4.3% H_2O_2 (v/v) at 75 °C for 10 min. The system was flushed with 2% (w/v) SDS and water before being dried with N_2 gas between treatments to avoid contamination. For each sample, the sensor was equilibrated in KP buffer at pH 7.2. Then, a 0.05 mg mL^{-1} solution of TMGMV-A or TMGMV-B in KP pH 7.2 was run at 150 µL min^{-1} until the sensor signal saturated (approximately 1 h for TMGMV-B and 2 h for TMGMV-A). The system was then flushed with KP pH 7.2 for 10 min to remove molecules that were loosely adsorbed. The IVN-A and IVN-B samples were diluted in KP pH 7.2 to 0.01 mg mL^{-1} and loaded onto the sensor at 150 µL min^{-1} until the sensor saturated, on the order of 1–2 h depending on the sample type. The system was then washed again with KP pH 7.2 for 10 min to remove ivermectin that was non-specifically bound. The output data was annotated to reflect the concentrations and flow rates of the samples, and the SmartFit algorithm in the QSense Dfind software was used to calculate the bound mass and thickness of the films.

Growth and maintenance of *C. elegans*

The N2 strain of *Caenorhabditis elegans* was obtained from Caenorhabditis Genetics Center (University of Minnesota; MN, USA), grown on solid Nematode Growth Medium (NGM) agar plates with OP-50 *E. coli* as the primary food source. The nematodes were grown and maintained at 20 °C in the dark.

Treatment of *C. elegans* and gel burrowing assay

As previously described, a solution of *C. elegans* was aliquoted with ~ 100 nematodes per microcentrifuge tube and concentrated for 30 s at 200 × g to create a pellet [17]. The supernatant was removed and replaced with one of the treatment group solutions ($N = 3$). The *C. elegans* were incubated for 90 min in these solutions before being transferred to the burrowing assay. Unless otherwise specified, treatment groups all contain 10 µM ivermectin as soluble drug or formulated as TMGMV nanoparticle. Some samples were applied directly, and another group was first passed through a soil

column prior to treatment of *C. elegans*. Using previously reported protocols, 26% (w/w) Pluronic F127 solutions were dissolved and kept on ice [17, 23]. Thirty microliters of Pluronic F127 was then added to a 6-well plate. Treated *C. elegans* were deposited on the droplet to introduce around 100 nematodes. After around 10 min, a layer of 2 mL Pluronic was cast on top. A solution of OP-50 *E. coli* lysate (20 µL of OD600 = 0.5) was added to the surface, and the nematodes were given 2 h to burrow before imaging. After 2 h, an 11 × 11 area scan at × 4 magnification (Keyence BZ-X800 Fluorescence Microscope) was taken for each well from the gel burrowing assay. The number of nematodes on the surface was counted manually, and the area fraction of their tracks was determined by edge detection and binary image transformation in ImageJ. Nematodes were also live imaged, and videos were recorded after treatment with several concentrations of ivermectin and ivermectin conjugates (0–10 µM).

Results and discussion

Using TMGMV as a testbed, we developed a biospecific ivermectin nanoparticle loading strategy. TMGMV labeled with biotin (TMGMV-B) and avidin (TMGMV-A) were prepared to bind either streptavidin-ivermectin (IVN-A) or biotin-ivermectin (IVN-B), respectively. The overall strategy is outlined in Fig. 1.

TMGMV-A was prepared as follows: TMGMV was purified using established protocols and reacted with 4-ethynylaniline by diazonium coupling to functionalize solvent-exposed tyrosines with alkyne groups (TMGMV-alk). The product was resuspended in HEPES buffer (pH 7.5, 20 mM). Avidin-N_3 was prepared by reacting the surface lysine of avidin (a tetrameric protein) with NHS-N_3. The reaction was optimized by varying the molar ratios of NHS-N_3 to avidin's lysines (2:1, 1:1, 1:2, and 1:4) and incubation time (30 min, 1 h, 2 h, and 24 h). Each of these preparations was then reacted with the TMGMV-alk at several ratios (2:1, 1:1, and 1:2 avidin to TMGMV

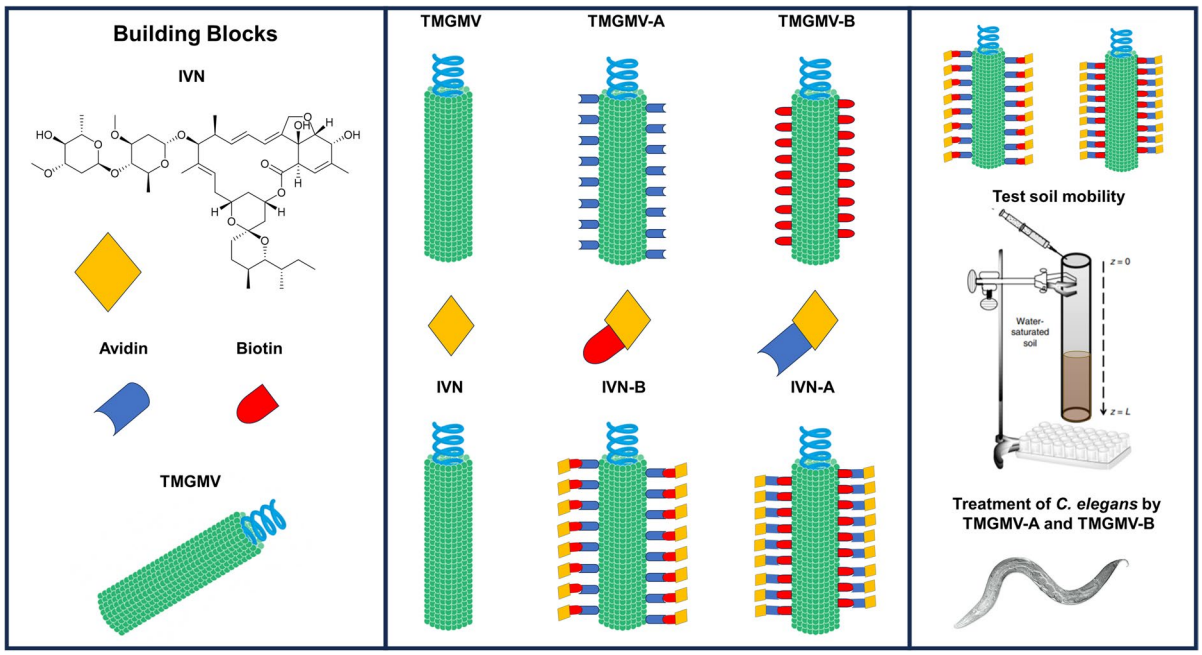

Fig. 1 The strategy of using biotin-avidin affinity for the loading of hydrophobic pesticides (here ivermectin = IVN) onto TMGMV for the treatment of nematodes (*C. elegans* was used as a model system). TMGMV is decorated with either avidin (blue) or biotin (red) to form TMGMV-A and TMGMV-B, respectively. IVN-biotin/streptavidin is introduced and forms a complex with its corresponding TMGMV-A/B; the complex is then used in efficacy assays against *C. elegans*. The blue helices represent RNA in the native viral nanoparticles

CP; each TMGMV consists of 2130 identical copies of a CP) for 30 min, 1 h, 2 h, or 24 h with the goal to maximize the functionalization of TMGMV with avidin groups via azide-alkyne cycloaddition to create TMGMV-A. The products were characterized and visualized on SDS-PAGE (Figure S1). The avidin monomer (16.4 kDa), TMGMV CP (17.5 kDa), TMGMV + avidin conjugate (~ 32 kDa), TMGMV CP dimers (35 kDa), and higher molecular weight aggregates were observed. Maximizing the amount of TMGMV + avidin (TMGMV-A) without creating larger molecular weight compounds would yield the most well-defined product: this was achieved by using a 2:1 molar excess of avidin-N_3 (synthesized using 1:1 NHS-azide per avidin lysine) per TMGMV-B incubated for 30 min. This formulation was then used for all further studies.

TMGMV-B was prepared using a previously established approach at 10 molar excess of biotin-N_3 to TMGMV coat proteins [22]. Using the optimized methods, TMGMV-A/B samples were prepared and analyzed on SDS-PAGE (Fig. 2A). Band analysis tool using ImageJ software indicates that 26.5% of the CPs of TMGMV-B were modified with biotin, and 12.5% of CP-A were quantified by ImageJ band analysis. The 12.5% however does not reflect the percentage of modified CP, because avidin is a tetramer. It is assumed that tetrameric avidin is bound to

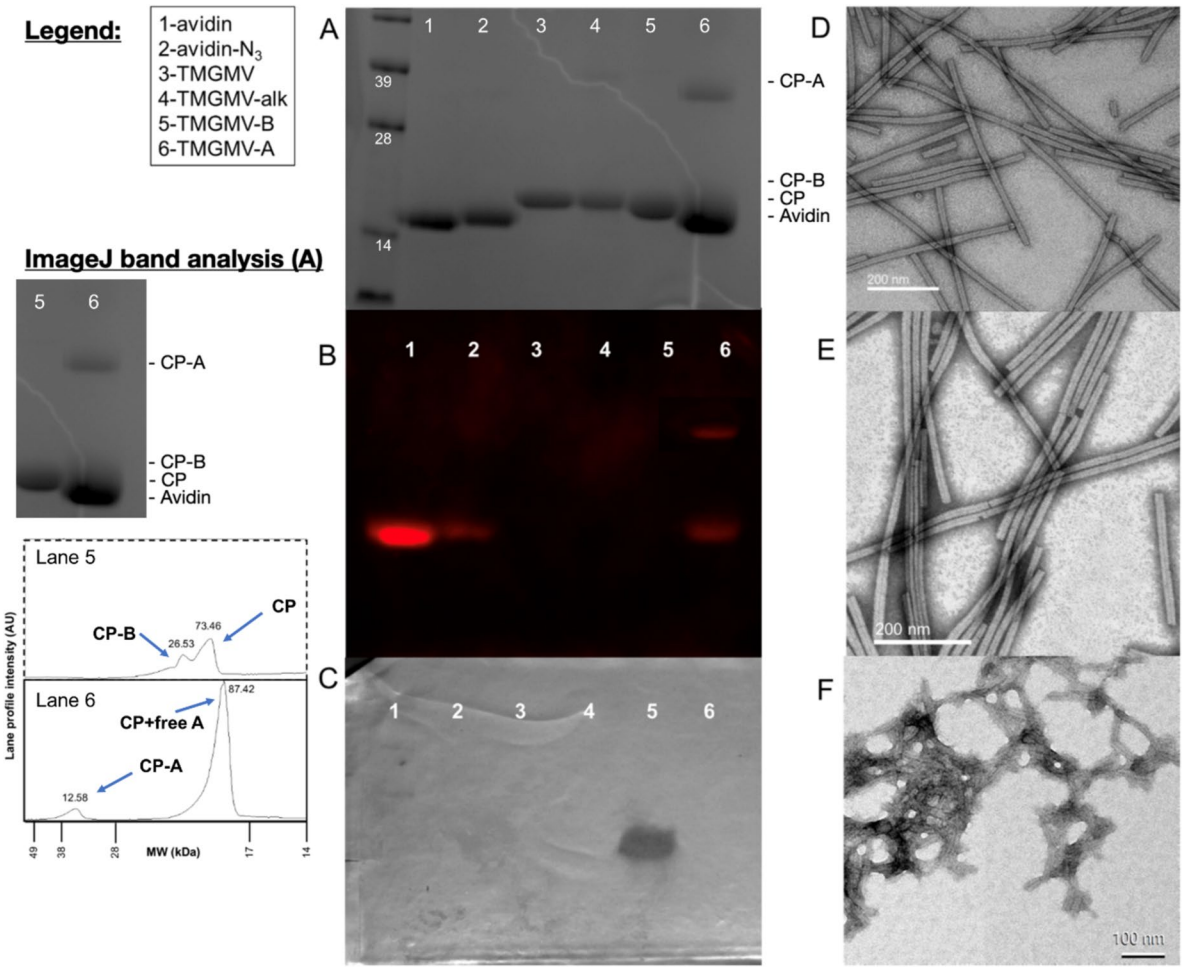

Fig. 2 Characterization of TMGMV, TMGMV-A, and TMGMV-B. The legend to the left describes what sample is in each lane (**A**–**C**) and details the ImageJ band analysis (**A**). **A** SDS-PAGE with the molecular weight markers (in kDa) listed. **B** Western blot with biotin-Cy5 labeling of avidin. **C** Western blot using anti-biotin HRP for detection of biotin. TEM micrographs of TMGMV (**D**), TMGMV-B (**E**), and TMGMV-A (**F**) with the scale bars shown at the bottom of the micrographs

TMGMV, but under the denaturing conditions of SDS-PAGE it dissociates into monomers—therefore, CP-A as well as a mixture of free avidin and CP is detected. Given the similar molecular weight of avidin monomer and CP (16.4 kDa and 17.5 kDa) and the relatively high amount of protein needed to detect TMGMV-A CP in the lane, the two bands cannot be deconvoluted. Hence, the mixture of CP and free avidin should be composed of ~ 37.5% avidin (3 × of CP-A) and ~ 62.5% unmodified CP. In other words, gel analysis indicates that ~ 550 biotin were conjugated per TMGMV-B and ~ 250 tetramers per TMGMV-A. These numbers are approximations; however, data are comparable to prior work using fluorescent dyes and similar bioconjugation chemistries on TMGMV [22].

To confirm the specific binding activity of TMGMV-A and TMGMV-B, the samples were transferred from SDS-PAGE to nitrocellulose membranes and treated with biotin-Cy5 (Fig. 2B) and anti-biotin HRP (Fig. 2C). The results indicate that there are specific interactions between avidin/avidin-N_3/TMGMV-A and biotin-Cy5 as well as anti-biotin HRP with TMGMV-B. Interestingly, the azide modification of avidin (Fig. 2B, lane 2) versus the unmodified avidin (Fig. 2B, lane 1) indicates that azide may quench or interfere with the biotin-Cy5 fluorescence on the TMGMV nanocarrier. This reduced fluorescence remains in the labeled TMGMV-A samples (Fig. 2B, lane 6), but with no further reduction in fluorescence. The lower band in this lane is associated with the non-conjugated avidin monomers which remain attached to the TMGMV in their tetrameric form but denature into monomers under SDS-PAGE conditions. Due to steric limitations, it is highly likely that only one of the four subunits covalently binds to the TMGMV-alkyne during the azide-alkyne cycloaddition reaction.

TEM micrographs of TMGMV (Fig. 2D), TMGMV-B (Fig. 2E), and TMGMV-A (Fig. 2F) show that, compared to native TMGMV or TMGMV-B, the TMGMV-A particles appear shorter in length (around 150–200 nm versus 300 nm) and have a propensity to aggregate under drying conditions. TMGMV-B appeared similar in morphology and shape to TMGMV. This data indicates that conjugation of the large protein-handle (i.e., avidin) may be less desired because this formulation tends to aggregate and break into shorter nanoparticles.

As a secondary point of validation, electrophoretic mobility shift assays of TMGMV, TMGMV-A, and TMGMV-B mixed with biotin and avidin samples were conducted. Each sample was incubated with either buffer, avidin, or 4-arm PEG biotin, and their mobility through an agarose gel was determined after 40 min at 120 V. Gels were stained with nucleic acid stain (to visualize TMGMV's nucleic acids, Figure S2A) and Coomassie Blue for staining of the TMGMV and avidin proteins (Figure S2B). Avidin samples were not detected, because samples migrated toward the cathode. TMGMV and TMGMV-B showed similar bands indicating the biotin label had no effect on the electrophoretic mobility; TMGMV-A has a broader distribution—which is consistent with broken and aggregated formulations as observed by TEM; further, the positive charge attributed by the conjugated avidin also likely impacts the electrophoretic properties of TMGMV-A.

TMGMV-A and TMGMV-B had reduced mobility when mixed with multivalent biotin and avidin, respectively. This is consistent with intermolecular interactions between TMGMV-A and biotin and TMGMV-B and avidin (Figure S2). As expected, TMGMV-A and TMGMV-B samples also interacted with one another, thus providing an opportunity to design networks of protein nanoparticles. Together data confirm that TMGMV-A and TMGMV-B nanoparticles were obtained, and their handles' functionality and binding to target molecules were confirmed.

Next, IVN was loaded onto TMGMV, and successful IVN loading was quantified and monitored using an ivermectin competitive ELISA as well as quartz crystal microbalance with dissipation (QCMD). A commercial ivermectin quantification ELISA kit was used (the standard curves as shown in Figure S3) to quantify IVN-B and IVN-A complexation with TMGMV-A and TMGMV-B, respectively (Fig. 3). We validated that the detection of IVN-A and IVN-B was not inhibited by their state of conjugation (Figure S3). The assay determined that TMGMV-A CP bound 63 μM of IVN-B and TMGMV-B CP bound 43 μM of IVN-A for a sample of 1 mg mL^{-1} TMGMV (57 μM CP). This amounts to ~ 1 IVN-B per TMGMV-A CP (~ 2000 IVN-B per TMGMV-A) and ~ 0.75 IVN-A per TMGMV-B CP (~ 1500 IVN-A per TMGMV-B). These values are overestimations or may indicate some free IVN in the samples, because the values exceed the theoretical loading capacity:

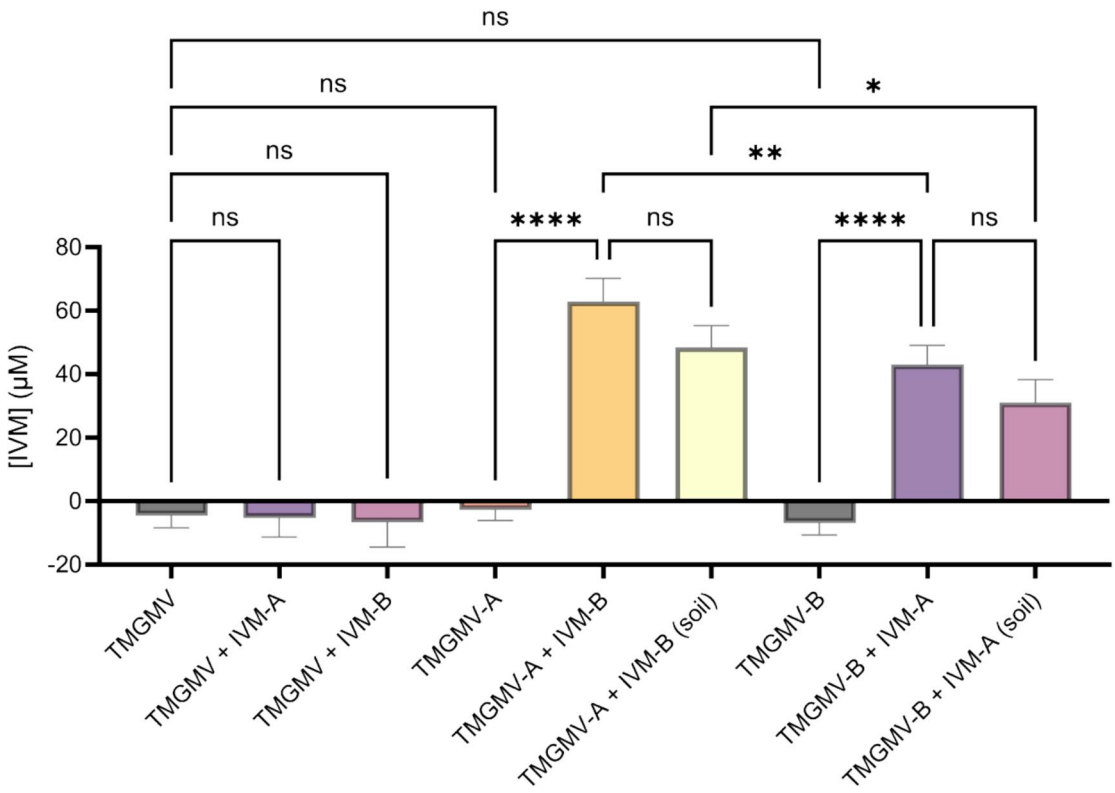

Fig. 3 Calculated ivermectin concentrations in each sample of TMGMV, TMGMV-A, and TMGMV-B after comparing their signal to the standard curves. Soil denotes samples that were subjected to soil columns prior to analysis. Statistical significance was determined using a multiple comparisons test ($N=3$). n.s. (no significance); *$p<0.1$, **$p<0.01$, ****$p<0.0001$

From Fig. 1A band analysis, we found that TMGMV-A has 250 tetramers attached with 4 binding sites per modified coat protein, hence offering ~ 1000 loading sites, and TMGMV-B displayed ~ 550 biotin sites per TMGMV particle.

Importantly, the cargo was stably retained on the TMGMV carrier when passing through soil: > 75% of ivermectin stays associated with TMGMV minimal cargo loss was observed (~ 1.35-fold reduction in bound IVN, but not statistically significant by multiple comparisons, Fig. 3).

The competitive ELISA is an indirect measurement but confirms the interaction between the viral nanocarriers and the intended cargo. The binding of IVN-A and IVN-B to TMGMV-A/B was verified by QCMD measurements (Fig. 4). TMGMV-A or TMGMV-B was loaded onto a gold sensor pre-incubated with buffer, and the signal was allowed to saturate. A wash-step using buffer was used to remove loosely bound protein, and then IVN-B or IVN-A were run over the sensor to allow for avidin–biotin interactions to occur. When the signal saturated, a buffer was used to wash loosely bound IVN off, and then the mass loading ratio was determined using the analysis software. The results are shown in Fig. 4B and D with surface mass density reported. For TMGMV-B, we found 3300 ng cm^{-2} of virus bound to the gold sensor and, when saturated with IVN-A, 5500 ng cm^{-2} were bound to the sensor. For TMGMV-A, after washing, 462 ng cm^{-2} were bound to the sensor, and after washing, 545 ng cm^{-2} when saturated with IVN-B. The calculated number of ivermectin per coat protein can be found using the following equation:

$$\text{mole ratio} = \frac{m_{\text{final}} - m_{\text{initial}}}{m_{\text{initial}}} \times \frac{\text{MW}_{\text{TMGMV}}}{\text{MW}_{\text{IVN}}}$$

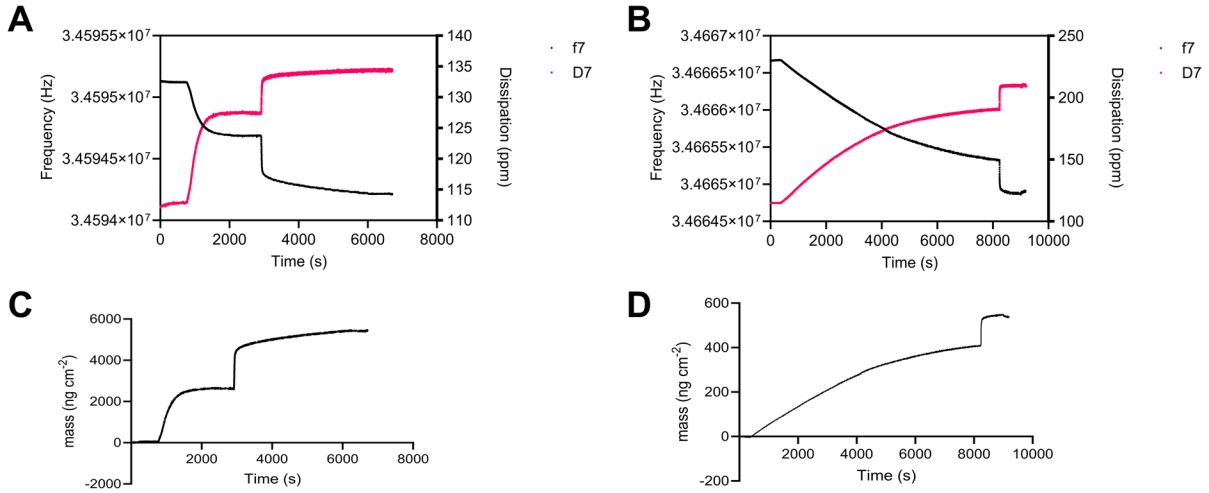

Fig. 4 QCM-D analysis of TMGMV-B with IVN-A (**A**) and TMGMV-A with IVN-B (**B**) for frequency and dissipation signals (**A**, **B**) and mass surface densities (**C**, **D**). **A**, **B** The horizontal axis denotes the time of each measurement, and the vertical axes denote the frequency (left axis) and dissipation (right axis) for each sample. **C**, **D** The vertical axis denotes mass density on the surface

The *m* values in the equation represent the final mass value after ivermectin washing and the initially bound TMGMV after washing. For each type of ivermectin, the molecular weight (MW_{IVN}) needs to reflect the size of the molecule (15,875 Da for IVN-A and 1120 Da for IVN-B). Using this equation, we find 0.734 IVN-A to TMGMV-B CP (1500 IVN-A per TMGMV-B) and 2.801 IVN-B to TMGMV-A CP (6000 IVN-B per TMGMV-A). Based on the degree of labeling of the TMGMV and the results from the ELISA and the QCM-D analysis, we can confirm there are non-specific but irreversible interactions between the TMGMV conjugates and the ivermectin which is more pronounced under QCM-D conditions. However, again, the results indicate that values are on overapproximation, because the degree of loading is higher than expected. Taken all together, despite a higher degree of non-specific binding on TMGMV-A with IVN-B, the improved solubility of IVN-A relative to IVN-B and the higher degree of labeling of TMGMV-B than TMGMV-A suggests the TMGMV-B/IVN-A approach may be more desirable for pesticide delivery applications.

With the overall goal being soil treatment to target plant parasitic nematodes, as a next step, we assessed soil mobility of the TMGMV-A and TMGMV-B conjugates. A soil column experiment was conducted using magic topsoil and established protocols [9, 13, 17]. TMGMV-A and TMGMV-B bound to their ivermectin counterparts did not show reduced mobility compared to TMGMV or TMGMV spherical nanoparticles (Fig. 5), with a maximum elution of 5.5 mL compared to 4 mL for TMGMV and 6.5 mL for TMGMV spherical nanoparticles under the same conditions. This corroborates prior findings that the relatively small size changes and relatively low surface modifications on TMGMV exhibited in

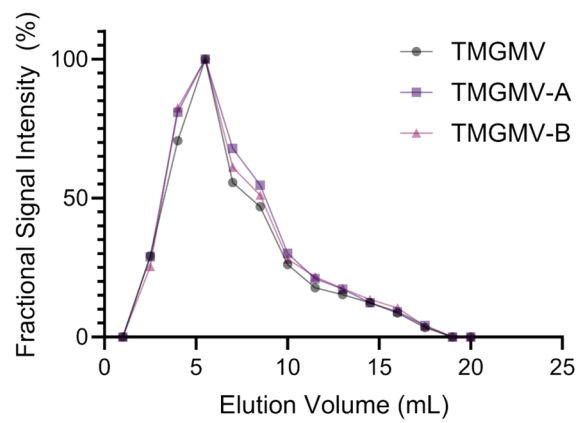

Fig. 5 Soil mobility profiles (determined by BCA signal) for TMGMV, TMGMV-A, and TMGMV-B in 10-mL soil columns with an irrigation rate of 5 mL $min.^{-1}$. Fractions of 1.5 mL were collected and analyzed using BCA assay to determine the protein content in each ($N=3$)

TMGMV-A and TMGMV-B do not drastically affect the soil mobility of TMGMV overall [13, 17].

As a final point, we tested the efficacy of the nanopesticides against *C. elegans*, a model organism for plant parasitic nematodes. The potency of IVN-A and IVN-B relative to IVN was compared using a video analysis of the nematodes (Supporting Videos). Each ivermectin compound was shown to paralyze the *C. elegans* after 90 min, indicating that the A/B labels do not impair its efficacy. Surface motility calculations were then conducted after 90 min of treatment with IVN, IVN-A, and IVN-B following previously established protocols [17].

Then nematodes were treated with TMGMV, the modified carriers TMGMV-A/B, and the carriers loaded with 10 μM ivermectin (TMGMV-A/B-IVN). The IVN loading was determined by ELISA; therefore, we note that this dose is likely an overestimation and/or presence of free IVN (see Figures 3 and 4). We compared the efficacy of TMGMV-A/B-IVN against free ivermectin, IVN-A, and IVN-B treatments at the same concentration. Nematodes were incubated with each of these samples for 90 min and then cast in an F-127 pluronic gel as previously described [17, 23]. If the nematodes were not paralyzed effectively by the ivermectin treatment, they would have burrowed through the gel to the surface where they are chemoattracted to *E. coli* lysate. The number of nematodes and area fraction of tracks on the surface was calculated using image processing with images. The detection of fewer nematodes means treatment was effective.

An example tile image showing *C. elegans* is shown in Figure S4, and the number of nematodes on the surface after 2 h of burrowing is shown in Fig. 6. The data show untreated samples; TMGMV, TMGMV-A, and TMGMV-B without any IVN have no statistical differences with an average of 71 ± 4.8 nematodes detected on the surface. The IVN treatment positive controls resulted in 26.5 ± 3.1 nematodes on the surface, while IVN-A led to 31 ± 2.3 nematodes and IVN-B led to 34 ± 3.7 nematodes. Our nanopesticide samples also led to a significant reduction in the number of nematodes with 39.5 ± 2.3 nematodes for TMGMV-A + IVN-B and 42.5 ± 3.8 nematodes for TMGMV-B + IVN-A. Thus, we can conclude that the conjugated ivermectin still is potent as a paralytic agent for *C. elegans* (SI videos). However, it is important to evaluate the efficacy of mimicking the indented soil application. Therefore, we first passed treatment samples through the soil and then applied the collected flow-through in the nematode efficacy assay as described above. From our prior work with IVN encapsulated in spherical nanoparticles (SNPs), we determined that free ivermectin is not effective because it lacks soil mobility—in stark contrast, IVN-laden SNPs were potent by enabling pesticide mobility in soil targeting the nematodes [17]. Like previous work with unconjugated ivermectin, IVN-A and IVN-B have no efficacy after passing through soil, demonstrating the necessity of a carrier to functionally deliver these conjugates through soil. In stark contrast, the nanopesticide formulations TMGMV-A + IVN-B and TMGMV-B + IVN-A demonstrated functional delivery and efficacy against nematodes. After passing through soil, TMGMV-A + IVN-B treated 38% of the nematodes (27 fewer nematodes on the surface) and TMGMV-B + IVN-A treated 31% of the nematodes (22 fewer nematodes on the surface) compared to the 71 nematodes measured in the untreated controls. When we consider changes in the efficacy of IVN treatment due to conjugation, IVN overestimation based on ELISA measurement, carrier binding, and passing through the soil (25% loss of cargo), we can see there are modest losses associated with each change. These are summarized in Table 1.

These results demonstrate that TMGMV-A and TMGMV-B each serve as a functional delivery vehicle of biotin or avidin-conjugated hydrophobic molecules in soil without the need for direct conjugation of the drug to the viral particle. This may have improved release behavior depending on the target organism for treatment due to the reversible nature of the biotin-(strept)avidin interaction and the affinity of ivermectin to soil particles. The release of 25% of the ivermectin after passing through the soil for both TMGMV-A and TMGMV-B suggests there may still be non-specifically bound ivermectin that is not fully binding to the functionalized TMGMV, and therefore, it exhibits a higher affinity for the soil than the viral nanoparticles. Taken in aggregate, the approach of using TMGMV-B with an avidin-functionalized pesticide may be most suitable for further development, because we observed solubility issues for the IVN-B compound; in contrast, conjugation of avidin enhanced solubility. Also, the TEM micrographs suggest the structural integrity of TMGMV-A was somewhat impaired with a high degree of particle

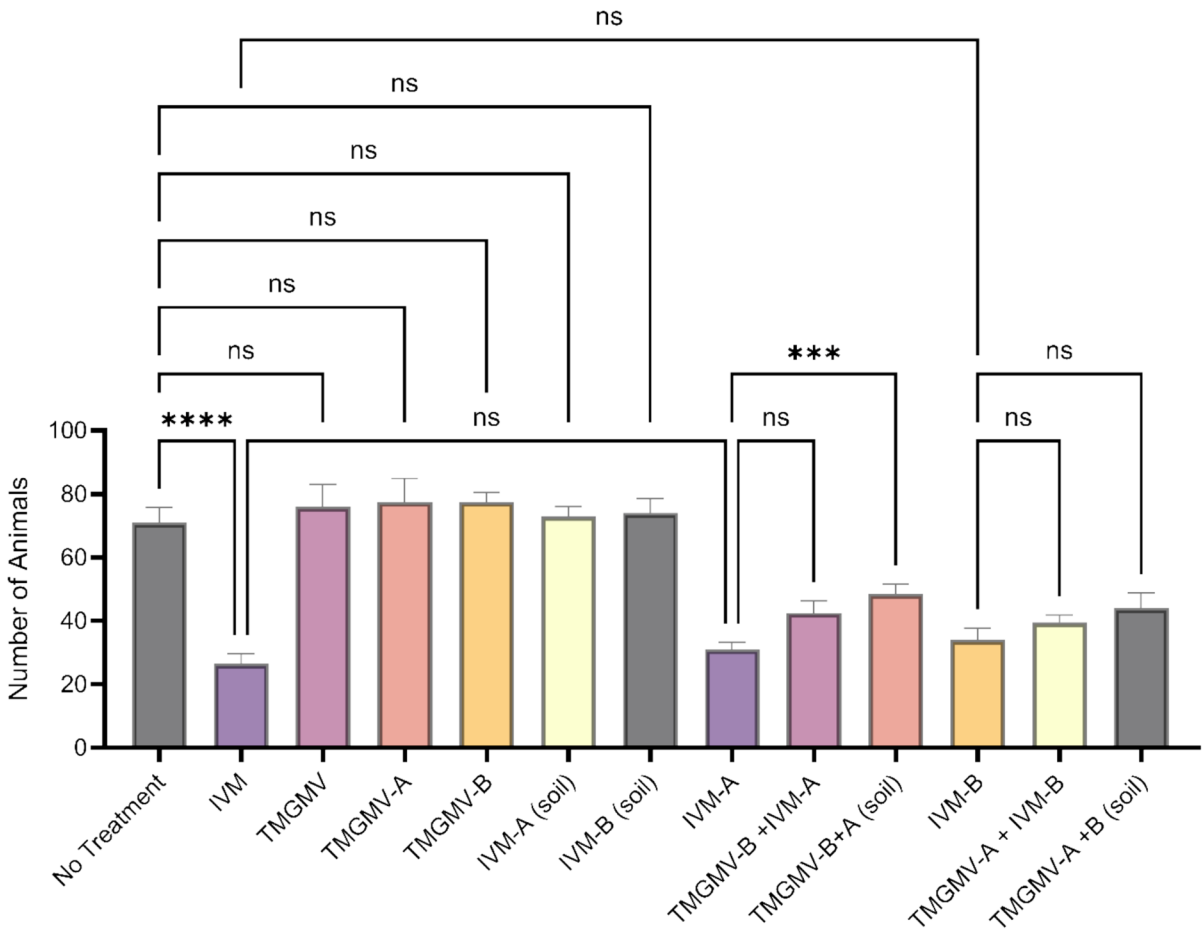

Fig. 6 The number of nematodes on the surface of a gel burrowing assays after 90 min of treatment and 2 h to burrow toward a chemoattractant on the surface. Statistical significance was determined using a multiple comparisons test ($N=3$). n.s. (no significance); ***$p<0.001$, ****$p<0.0001$

Table 1 Fold change in the efficacy of IVN treatment relative to free IVN in vitro (62% reduction in nematodes)

	IVN conjugate (in vitro)	IVN formulation with TMGMV-B/A carrier (in vitro)	IVN formulation with TMGMV-B/A (through soil)
IVN-A	0.89 (56% reduction)	0.71 (44% reduction)	0.61 (38% reduction)
IVN-B	0.83 (52% reduction)	0.64 (40% reduction)	0.49 (31% reduction)

breakage. In all cases where nematodes were exposed to TMGMV, TMGMV-A, TMGMV-B, or SNPs, *C. elegans* was observed by microscopy to chemotactically target and feed on virus-derived materials, suggesting the virus carriers may shield the nematodes from identifying ivermectin as a toxic compound. When compared to the SNPs, this approach does have some drawbacks. SNPs were able to overcome the loss of efficacy in soil by reformulating the particles and also had a higher mass loading of ivermectin. However, this biotin/avidin coupling approach does not require cosolvents or near-boiling conditions to achieve the loading of the active molecule, which may be particularly advantageous for heat-sensitive

molecules. When considering the adoption of a new technology in an agricultural setting, keeping costs and processing steps as low as possible and the drug-to-carrier ratio high is paramount. While this platform demonstrates nematicidic efficacy against *C. elegans* after soil delivery, there is still room for improvement to create a field-ready technology for plant-parasitic nematode treatment.

Conclusions

TMGMV-A and TMGMV-B each successfully demonstrated their potential as an agrochemical delivery vehicle. In terms of performance, both constructs were shown to effectively load IVN-B and IVN-A, respectively, at a dose that could be used to treat *C. elegans*. The biotin/avidin-modified TMGMV carriers maintained soil mobility and enabled nematode killing in the burrowing assay, while free ivermectin had no efficacy. In particular, TMGMV-B with IVN-A proves to be the more promising formulation for future studies. These data compare well with the thermal encapsulation approach in SNPs, demonstrating a parallel design strategy for hydrophobic cargo loading that does not require heat and may be useful for more sensitive or heat-labile agrochemical targets.

Acknowledgements The authors thank the University of California, San Diego-Cellular and Molecular Medicine Electron Microscopy Core (UCSD-CMM-EM Core, RRID: SCR_022039) for equipment access and technical assistance. The UCSD-CMM-EM Core is partly supported by the National Institutes of Health Award number S10OD023527. The authors acknowledge Majid Ghassemian of the Biomolecular and Proteomics Mass Spectrometry Facility (BPMSF) at the University of California, San Diego, for his assistance and use of facilities. The BPMSF is funded by the NIH under grants S10 OD016234 (Synapt-HDX-MS) and S10 OD021724 (LUMOS Orbi-Trap). This work was performed in part at the San Diego Nanotechnology Infrastructure (SDNI) of the University of California, San Diego, a member of the National Nanotechnology Coordinated Infrastructure (NNCI), which is supported by the National Science Foundation (grant ECCS-1542148). This work was performed in part at the University of California, San Diego, Department of Neurosciences Microscopy Core, supported by the National Institutes of Health (NINDS P30NS047101).

Author contribution The manuscript was written through contributions of all authors. All authors have given approval to the final version of the manuscript. AAC: design of experiments, method development, nematode maintenance, image analysis, immunosorbent assays, nematode treatment, nanomaterial characterization, manuscript writing; SCL: nematode maintenance, gel electrophoresis, nanocarrier formulation; IGG: gel analysis, method development, immunostaining; NFS: conceptualization, supervision, funding acquisition, editing of manuscript.

Funding This work was supported by a grant from USDA NIFA-2020–67021-31255 (to NFS) and USDA NIFA-2022–67012-36698 (to AAC). This work was sponsored in part by the UC San Diego Materials Research Science and Engineering Center (UCSD MRSEC), supported by the National Science Foundation Grant DMR-2011924 (to NFS).

Data availability Data is provided within the manuscript and supporting information files. Source images for analysis may be available upon request to AAC or NFS.

Declarations

Conflict of interest The authors declare the following competing financial interest(s): Dr. Steinmetz is a co-founder of, has equity in, and has a financial interest with Mosaic ImmunoEnginering Inc. Dr. Steinmetz is a co-founder of, and serves as manager of Pokometz Scientific LLC, under which she is a paid consultant to Mosaic as well as Flagship Pioneering (FL95 and Arana Bioscience). The other authors declare no potential COI.

References

1. Arias-Estévez M, López-Periago E, Martínez-Carballo E, Simal-Gándara J, Mejuto J-C, García-Río L (2008) The mobility and degradation of pesticides in soils and the pollution of groundwater resources. Agric Ecosyst Environ 123(4):247–260. https://doi.org/10.1016/j.agee.2007.07.011
2. Brewer A, Dror I, Berkowitz B (2020) The mobility of plastic nanoparticles in aqueous and soil environments: a critical review. ACS ES&T Water 1(1):48–57. https://doi.org/10.1021/acsestwater.0c00130

3. Singh S, Singh B, Singh AP (2015) Nematodes: a threat to sustainability of agriculture. Proc Environ Sci 29:215–216. https://doi.org/10.1016/j.proenv.2015.07.270
4. Katagi T (2013) Soil column leaching of pesticides, in Reviews of environmental contamination and toxicology volume 221, Whitacre DM Ed. New York, NY: Springer New York, pp 1–105
5. Anderson B, Phillips B, Hunt J, Largay B, Shihadeh R, Tjeerdema R (2011) Pesticide and toxicity reduction using an integrated vegetated treatment system. Environ Toxicol Chem 30(5):1036–1043. https://doi.org/10.1002/etc.471
6. Bexfield LM, Belitz K, Lindsey BD, Toccalino PL, Nowell LH (2020) Pesticides and pesticide degradates in groundwater used for public supply across the United States: occurrence and human-health context. Environ Sci Technol 55(1):362–372. https://doi.org/10.1021/acs.est.0c05793
7. Opdensteinen P, Charudattan R, Hong JC, Rosskopf EN, Steinmetz NF Biochemical and nanotechnological approaches to combat phytoparasitic nematodes. Plant Biotechnol J. https://doi.org/10.1111/pbi.14359
8. Beckers SJ, Staal AHJ, Rosenauer C, Srinivas M, Landfester K, Wurm FR (2021) Targeted drug delivery for sustainable crop protection: transport and stability of polymeric nanocarriers in plants. Adv Sci 8(11):2100067. https://doi.org/10.1002/advs.202100067
9. Chariou PL, Dogan AB, Welsh AG, Saidel GM, Baskaran H, Steinmetz NF (2019) Soil mobility of synthetic and virus-based model nanopesticides. Nat Nanotechnol 14(7):712–718. https://doi.org/10.1038/s41565-019-0453-7
10 Chariou PL, Steinmetz NF (2017) Delivery of pesticides to plant parasitic nematodes using tobacco mild green mosaic virus as a nanocarrier. ACS Nano 11(5):4719–4730. https://doi.org/10.1021/acsnano.7b00823
11. Cao J, Guenther RH, Sit TL, Lommel SA, Opperman CH, Willoughby JA (2015) Development of abamectin loaded plant virus nanoparticles for efficacious plant parasitic nematode control. ACS Appl Mater Interfaces 7(18):9546–9553. https://doi.org/10.1021/acsami.5b00940
12. Cao J, Guenther RH, Sit TL, Opperman CH, Lommel SA, Willoughby JA (2014) Loading and release mechanism of red clover necrotic mosaic virus derived plant viral nanoparticles for drug delivery of doxorubicin. Small 10(24):5126–5136. https://doi.org/10.1002/smll.201400558
13. Venkateswaran UP, Caparco AA, González-Gamboa I, Caballero RM, Schuphan J, Steinmetz NF (2023) Plant viral nanocarrier soil mobility as a function of soil type and nanoparticle properties. ACS Agric Sci Technol 3(7):583–592. https://doi.org/10.1021/acsagscitech.3c00074
14. Decraemer W, Robbins RT (2007) "The who, what and where of longidoridae and trichodoridae", (in Eng). J Nematol 39(4):295–297
15. Everaert EA, Viaene N, Quataert P, Haegeman A, De Jonghe K (2024) Towards improved nepovirus detection and identification in Xiphinema nematodes. PhytoFrontiers™: pp PHYTOFR-03–24–0018-R. https://doi.org/10.1094/phytofr-03-24-0018-r
16. Charudattan R, Hiebert E (2007) A plant virus as a bioherbicide for tropical soda apple, Solanum viarum. Outlooks Pest Manag 18(4):161–171. https://doi.org/10.1564/18aug07
17 Caparco AA, González-Gamboa I, Hays SS, Pokorski JK, Steinmetz NF (2023) Delivery of nematicides using TMGMV-derived spherical nanoparticles. Nano Lett 23(12):5785–5793. https://doi.org/10.1021/acs.nanolett.3c01684
18. Guenther RH, Lommel SA, Opperman CH, Sit TL (2018) Plant virus-based nanoparticles for the delivery of agronomic compounds as a suspension concentrate, in Virus-derived nanoparticles for advanced technologies: methods and protocols, vol. 1776. New York, NY: Springer New York, pp 203–214
19 Gerhardson B, Insunza V (1979) Soil transmission of red clover necrotic mosaic virus. J Phytopathol 94(1):67–71. https://doi.org/10.1111/j.1439-0434.1979.tb04219.x
20. Shin MD, Hochberg JD, Pokorski JK, Steinmetz NF (2021) Bioconjugation of active ingredients to plant viral nanoparticles is enhanced by preincubation with a Pluronic F127 polymer scaffold. ACS Appl Mater Interfaces 13(50):59618–59632. https://doi.org/10.1021/acsami.1c13183
21. González-Gamboa I et al (2024) Inter-coat protein loading of active ingredients into tobacco mild green mosaic virus through partial dissociation and reassembly of the virion. Sci Rep 14(1):7168. https://doi.org/10.1038/s41598-024-57200-0
22. González-Gamboa I, Caparco AA, McCaskill JM, Steinmetz NF (2022) Bioconjugation strategies for tobacco mild green mosaic virus. ChemBioChem 23(18):e202200323. https://doi.org/10.1002/cbic.202200323
23. Lesanpezeshki L et al (2019) Pluronic gel-based burrowing assay for rapid assessment of neuromuscular health in C. elegans. Sci Rep 9(1):15246. https://doi.org/10.1038/s41598-019-51608-9